Molecular Biology of the Cell
Vol. 11, 79–91, January 2000

# Myosin-II Tails Confer Unique Functions in *Schizosaccharomyces pombe*: Characterization of a Novel Myosin-II Tail

**Magdalena Bezanilla*† and Thomas D. Pollard†‡**

*Biochemistry Cellular and Molecular Biology Graduate Program, Johns Hopkins University School of Medicine, Baltimore, Maryland 21205; and †Structural Biology Laboratory, The Salk Institute for Biological Studies, La Jolla, California 92037

Submitted August 3, 1999; Revised November 3, 1999; Accepted November 4, 1999
Monitoring Editor: David Drubin

*Schizosaccharomyces pombe* has two myosin-IIs, Myo2p and Myp2p, which both concentrate in the cleavage furrow during cytokinesis. We studied the phenotype of mutant myosin-II strains to examine whether these myosins have overlapping functions in the cell. *myo2*$^+$ is essential. *myp2*$^+$ cannot rescue loss of *myo2*$^+$ even at elevated levels of expression. *myp2*$^+$ is required under specific nutritional conditions; thus *myo2*$^+$ cannot rescue under these conditions. Studies with chimeras show that the tails rather than the structurally similar heads determine the gene-specific functions of *myp2*$^+$ and *myo2*$^+$. The Myo2p tail is a rod-shaped coiled-coil dimer that aggregates in low salt like other myosin-II tails. The Myp2p tail is monomeric in high salt and is insoluble in low salt. Biophysical properties of the full-length Myp2p tail and smaller subdomains indicate that two predicted coiled-coil regions fold back on themselves to form a rod-shaped antiparallel coiled coil. This suggests that Myp2p is the first type II myosin with only one head. The C-terminal two-thirds of Myp2p tail are essential for function in vivo and may interact with components of the salt response pathway.

## INTRODUCTION

Type II myosins are the best characterized members of the myosin family, essential for muscle contraction and for cytokinesis (Satterwhite and Pollard, 1992; Fishkind and Wang, 1995). All characterized myosin-IIs have heads with similar ATPase mechanisms. The tails are rod-shaped coiled coils of two parallel alpha-helices, resulting in a myosin with two heads on one end of the tail. Tails assemble into bipolar filaments with molecules staggered by 15 nm (Pollard, 1982; Huxley and Brown, 1967). During cytokinesis myosin-II is required to constrict the contractile ring (Mabuchi and Okuno, 1977). Contraction of an actomyosin system such as a muscle cell or a contractile ring requires sliding of actin filaments past each other via a bipolar myosin-II filament.

Of the unicellular organisms such as *Acanthamoeba*, *Dictyostelium*, and *Saccharomyces cerevisiae*, where myosin-II has been cloned and or biochemically isolated (Watts *et al.*, 1987; Sellers *et al.*, 1996), *Schizosaccharomyces pombe* is unique in that it has two myosin-IIs, Myo2p (Kitayama *et al.*, 1997; May *et al.*, 1997) and Myp2p (Bezanilla *et al.*, 1997; Motegi *et al.*, 1997). Their functions have been deduced from genetic studies. Myo2p is required for viability, and loss leads to a defect in cytokinesis. Myp2p is required for cytokinesis under specific nutritional conditions. Both myosins localize to the contractile ring during cytokinesis (Bezanilla *et al.*, 1997; Kitayama *et al.*, 1997). Are these myosins simply redundant? Myo2p and Myp2p have very similar catalytic domains but quite different tails. Myo2p has a short tail (711 residues), which is predicted to be almost entirely alpha-helical. Myp2p has a long tail (1336 residues) with two predicted coiled-coil regions separated by 250 amino acids.

Our studies of the phenotypes of mutant myosin-II strains show that the two myosins have unique functions in *S. pombe*. The tails of these myosins define their gene-specific functions. The Myo2p tail is similar to well-characterized myosin-II tails; however, the properties of the Myp2p tail are unprecedented. We also mapped specific regions of the Myp2p tail required for its function in vivo. These results suggest distinct roles for these proteins in fission yeast.

## MATERIALS AND METHODS

### *Strains, Media, and Transformation*

Table 1 lists *S. pombe* strains used in this study. Yeast culture, methods, media, and genetic manipulations were carried out by standard methods (Moreno *et al.*, 1991). Transformation of *S. pombe*

‡Corresponding author. E-mail address: pollard@salk.edu.

**Table 1.** Strains used in this study

| Strain | Genotype |
|---|---|
| FY435 | *h*$^+$ *his7-366 leu1-32 ura4-D18 ade6-M210* |
| FY436 | *h*$^-$ *his7-366 leu1-32 ura4-D18 ade6-M216* |
| TP5 | *h*$^-$ Δ*myp2*::*his7*$^+$ *his7-366 leu1-32 ura4-D18 ade6-M210* |
| TP50 | *h*$^+$ Δ*myp2*::*his7*$^+$ *his7-366 leu1-32 ura4-D18 ade6-M216* |
| TP65 | *h*$^+$ Δ*myo2*::*ura4*$^+$ *his7-366 leu1-32 ura4-D18 ade6-M216* |
| | *h*$^-$ *myo2*$^+$ *his7-366 leu1-32 ura4-D18 ade6-M210* |
| TP73 | *h*$^-$ *myo2-E1 his7-366 leu1-32 ura4-D18 ade6-M216* |
| TP74 | *h*$^-$ Δ*myp2*::*his7*$^+$ *myo2-E1 his7-366 leu1-32 ura4-D18 ade6-M216* |
| TP81 | *h*$^+$ Δ*myp2*::*his7*$^+$ Δ*myo2*::*ura4*$^+$ *his7-366 leu1-32 ura4-D18 ade6-M216* |
| | *h*$^-$ *myp2*$^+$ *myo2*$^+$ *his7-366 leu1-32 ura4-D18 ade6-M210* |
| TP83 | *h*$^-$ Δ*myo2*::*ura4*$^+$ *his7-366 leu1-32 ura4-D18 ade6-M216* [pGFP-myo2] |
| TP86 | *h*$^-$ Δ*BC*::*ura4*$^+$ *his7-366 leu1-32 ura4-D18 ade6-M216* |
| TP87 | *h*$^-$ Δ*C*::*ura4*$^+$ *his7-366 leu1-32 ura4-D18 ade6-M216* |

was achieved by electroporation (Moreno *et al.*, 1991) or by a lithium acetate method (Okazaki *et al.*, 1990).

## Construction of Disruption Strains

To disrupt *myo2*$^+$, we inserted *ura4*$^+$, a 1.8-kb fragment from pTZura4 (a kind gift from S.L. Forsburg, The Salk Institute for Biological Studies, La Jolla, CA), between 461 and 4058 bp of *myo2*$^+$ corresponding to residues 154 and 1353, removing 80% of the open reading frame. The disruption construct contained an additional 436 bp of 3′ noncoding region. We transformed the linear construct into an *ura4-D18* wild-type diploid constructed from FY435 and FY436. We sporulated Ura$^+$ transformants on Edinberg minimal media (EMM) and analyzed stably transformed Ura$^+$ haploids by PCR (Bezanilla *et al.*, 1997) to determine the position of integration of the *ura4*$^+$ gene.

To construct Δ*myp2* Δ*myo2* (TP81), we transformed strain TP65 with the complementing plasmid pGFPmyo2, which carries the strongest *nmt1*$^+$ promoter (Tommasino and Maundrell, 1991; Basi *et al.*, 1993) and the nutritional marker *LEU2*. We sporulated the transformed diploid and selected for Ura$^+$ and Leu$^+$ spores, containing the disruption and the plasmid (TP83). We crossed TP83 with TP50 to construct a diploid, selected for loss of the plasmid pGFP-myo2; the resulting strain is TP81.

To construct the disruption of the *myp2*$^+$ tail, we used the Ntail construct described below and the NB (residues 828-1610, amplified by PCR) construct (both contain in-frame stop codons) and cloned them upstream of *ura4*$^+$. A 3′ region of *myp2*$^+$ from 6271 to 7381 bp, 1064 bp downstream of the stop codon, was cloned downstream of *ura4*$^+$. We transformed the linear disruption constructs into strain FY436. Stable Ura$^+$ transformants were analyzed by PCR (Bezanilla *et al.*, 1997) to determine the position of integration of the *ura4*$^+$ gene.

## Construction of Chimeric Myosins

We designed primers to amplify sequences encoding the heads and tails of *myo2*$^+$ and *myp2*$^+$. The 3′ primer for the head of each myosin contained a silent single-point mutation converting the sequence CCTTGG to CCATGG introducing an *Nco*I restriction enzyme site. The heads consisted of residue 2 to the residue preceding an invariant proline (residue 814 for Myo2p and residue 826 for Myp2p) at the beginning of the coiled-coil rod. The 5′ primer for the *myp2*$^+$ tail contains sequence from the 3′ end of the *myo2*$^+$ head including the engineered *Nco*I site. The 5′ primer for the *myo2*$^+$ tail contains sequence from the 3′ end of the *myp2*$^+$ head including the engineered *Nco*I site. Using the unique *Nco*I site we ligated the *myp2*$^+$ tail PCR product to the *myo2*$^+$ head PCR product and vice versa. These constructions were accomplished in a shuttle vector. The final chimera lacking the start methionine was then cloned into an expression vector.

## Complementation and Overexpression

The expression vectors are all N-terminal green fluorescent protein (GFP)-tagging vectors that carry the thiamine-repressible *nmt1*$^+$ promoter. The vectors in Figure 2A were constructed for this study and have the *LEU2* nutritional marker and carry the wild-type *nmt1*$^+$ promoter (strongest, derived from pRep4; Tommasino and Maundrell, 1991). The vectors in Figure 2B are based on pSGP573 (a gift from S.G. Pasion, The Salk Institute for Biological Studies, La Jolla, CA) and have the *ura4*$^+$ nutritional marker and carry the strongest *nmt1*$^+$ promoter. The vectors in Table 3 were constructed for this study and have the *LEU2* nutritional marker and carry a mutant *nmt1*$^+$ promoter (weakest, derived from pRep82) with a mutation in the TATA box, which reduces expression from the promoter (Basi *et al.*, 1993).

Myosin derivatives cloned into various expression vectors were transformed into strains (complementation of Δ*myo2* strains described below) as indicated in Table 3 and Figure 2. For all haploid strains, either Leu$^+$ or Ura$^+$ transformants were selected and then streaked to selective EMM with or without thiamine. The transformants with the strongest overexpression phenotype (without thiamine) were chosen for subsequent complementation experiments on the assumption that this selected for transformants with the highest level of basal expression in the presence of thiamine. This also resulted in transformants with relatively similar levels of expression, as verified by immunoblotting for the GFP tag (our unpublished results). Complementation was tested in the presence of thiamine under the conditions shown in Table 3 and Figure 2. For complementation of Δ*myo2* or Δ*myo2* Δ*myp2*, we transformed strains TP65 and TP81, respectively. Leu$^+$ transformants were selected and tested for an overexpression phenotype. Diploid transformants that exhibited a phenotype without thiamine were selected for complementation studies (for reasons described above). We sporulated the diploid and selected for cells containing the disruption(s) and plasmid by plating on selective media with thiamine at 32°C. We verified the ploidy of the resulting colonies by flow cytometry (Liang *et al.*, 1999). Cells overexpressing myosins were grown in 0.05 μM thiamine, a lower concentration of thiamine that results in an intermediate level of expression (Javerzat *et al.*, 1996), resulting in a larger number of viable cells.

Myo2p Tail, Myp2p Tail, and Myp2p tail subdomain constructs were amplified by PCR (see Figure 4). An *Nde*I site was engineered

into the 5′ primer, and a *Bam*HI site was engineered into the 3′ primer. Myo2p Tail starts at residue 816, which is the residue following the invariant proline. Myp2p Tail starts at residue 828, the analogous residue to the start site in Myo2p Tail. The following Myp2p tail subdomain constructs contain residues Ntail (828–1247) and Ctail (1610–2104). An in-frame stop codon was also engineered into the 3′ primer for the Ntail construct. The engineered sites were then used to clone the PCR products into pMW172 (Way *et al.*, 1990) for expression in bacteria.

### Expression and Purification of Myosin Tail Constructs

Plasmids for the myosin tail constructs were transformed into bacteria BL21-DE3 cells (Stratagene, La Jolla, CA). A 250-ml culture was inoculated and grown for at least 18 h at 37°C. Cells were harvested by centrifugation and lysed by sonication in lysis buffer: 20 mM imidazole, pH 7, 25% sucrose, 10 mM EDTA, 1 mM DTT, 1 mM PMSF, 200 μM leupeptin, 200 μM antipain, 5 μM pepstatin, 100 μM $N^{\alpha}$-tosyl-phe chloromethyl ketone, and 1 mM Pefabloc (Roche Molecular Biochemicals, Manheim, Germany). The lysate was cleared by centrifugation at 100,000 × *g* for 30 min. The pellet was solubilized in TED buffer (20 mM Tris, pH 7.5, 1 mM EDTA, 1 mM DTT) with 2 M urea and 1 mM PMSF in a tight Dounce homogenizer and spun at 100,000 × *g* for 15 min. The supernatant was discarded, and the pellet was solubilized in TED buffer with 4 M urea and 1 mM PMSF in a tight Dounce homogenizer. The solution was spun at 100,000 × *g* for 15 min. The supernatant was loaded unto a DEAE-Sepharose column, washed with 2 column volumes of TED buffer with 4 M urea, and then eluted with a NaCl gradient in TED buffer with 4 M urea from 0 to 100 mM NaCl. The eluted protein was diluted to a concentration of <0.1 mg/ml and dialized against TED buffer with 2 M urea and 250 mM NaCl (for Myo2p Tail) or 500 mM NaCl (for all Myp2p tail constructs). The proteins were slowly dialized out of urea by two changes of buffer per day so that the concentration of urea fell from 2 to 1, 0.5, 0.25, and 0 M urea. The resulting protein was spun at 100,000 × *g* for 30 min, and the supernatant was concentrated using centriprep concentrators (Amicon, Beverly, MA).

### Light Microscopy

For analysis of the phenotypes of the mutant myosin-II strains, cells were grown to midlog phase in YES media at 25°C, and then half of the culture was shifted to 36°C. After 4 h, the cells were harvested by centrifugation at 3000 rpm for 5 min in a swinging bucket table-top centrifuge (Beckman Instruments, Palo Alto, CA). Cells were fixed by vortexing the pellet in cold 70% ethanol. Cells were pelleted and resuspended in PBS containing 1 μg/ml DAPI for 10 min in the dark. Cells were pelleted, resuspended in PBS, and mounted on a microscope slide with a coverslip. Cells were observed with a 100× objective on an Olympus (Tokyo, Japan) inverted microscope by differential interference contrast and fluorescence using a DAPI filter.

To determine the localization of the GFP-myosin construct in overexpressing cells, cells were grown on plates containing 0.05 μM thiamine, a low level of thiamine allowing detection of the overexpression phenotype (Javerzat *et al.*, 1996) before the cells die. Cells were removed from the plate, resuspended in PBS, and mounted on a microscope slide with a coverslip. Cells were observed with a 63× objective on a Leitz (Wetzlar, Germany) microscope using a filter appropriate for GFP fluorescence. Images were photographed with 35-mm slide film, digitally scanned, and printed using Adobe (Mountain View, CA) Photoshop.

### Electron Microscopy

Purified Myo2p Tail and Myp2p Tail at 2 μM in TED buffer with 250 mM NaCl (Myo2p Tail) or 500 mM NaCl (Myp2p Tail) were mixed 1:1 with glycerol and sprayed onto freshly cleaved mica. After drying in a vacuum, the mica was rotary shadowed with platinum and carbon and viewed in the electron microscope (Sinard and Pollard, 1989). Negatives of micrographs taken at 31,500× were digitally scanned and printed using Adobe Photoshop.

### Analytical Ultracentrifugation

Sedimentation velocity and equilibrium runs were carried out at 20°C using An-60 Ti rotor in a Beckman Optima XLI ultracentrifuge using absorbance optics at 280 nm. For sedimentation equilibrium, we loaded Myp2p Tail, Myo2p Tail, Ntail, and Ctail into a six-hole, charcoal-filled Epon centerpiece and centrifuged them to equilibrium (at least 15 h at each speed). We collected data sets every hour. We determined the root mean square deviation of each data set from the final using Matchv7 software (Jeff Lary, National Analytical Ultracentrifuge Facility, Storrs, CT), and considered equilibrium attained when there was no change in root mean square deviation in consecutive data sets. We used the program Reedit9 (Jeff Lary) to truncate and save the data for individual samples into separate data sets. We determined the effective reduced molecular weight of each protein from a global fit of all data sets with the program Winonln (Johnson *et al.*, 1981).

For sedimentation velocity, we loaded Ntail, Ctail, and Ntail+Ctail in TED buffer with 500 mM NaCl into a two-sector, charcoal-filled Epon centerpiece and centrifuged at 40,000 rpm at 20°C for ~4 h. We collected data sets every 2 min. We determined the sedimentation coefficient with the programs Svedberg (John Philo, Amgen, Thousand Oaks, CA) and DCDT (Walter Stafford, Boston Biomedical Research Institute, Boston, MA).

### Phylogenetic Analysis

Myosin-II sequences were obtained from GenBank and are listed in Table 5, along with the sequence ID number. We constructed the alignments and built the trees as previously described (Bezanilla *et al.*, 1997).

## RESULTS

### The Two Myosin-IIs in S. pombe Have Distinct Functions

*S. pombe* has genes for two myosin-IIs. To determine whether these myosin-IIs have unique or redundant functions, we investigated the phenotypes of mutant myosin-II strains. Previous studies showed that the deletion Δ*myo2* is lethal (Kitayama *et al.*, 1997; May *et al.*, 1997) and that the deletion Δ*myp2* is essential under specific nutritional conditions (Bezanilla *et al.*, 1997). Balasubramanian *et al.* (1998) isolated a temperature-sensitive allele of *myo2*$^{+}$, *myo2-E1*, in a screen for cytokinesis mutants. The phenotype of *myo2-E1* is interesting, because the strain is temperature sensitive only in rich media (Figure 1B and Table 2). Under other media conditions, specifically in 1 M KCl (Figure 1B) or in minimal media (Table 2), *myo2-E1* is viable at all temperatures. Loss of *myp2*$^{+}$ function is without phenotype in rich media but gives a cytokinesis phenotype in minimal media and in 1 M KCl (Bezanilla *et al.*, 1997; Table 2), suggesting a novel function for *myp2*$^{+}$. That *myp2*$^{+}$ is required under conditions in which *myo2-E1* is not suggests that *myp2*$^{+}$ may rescue *myo2-E1* under these conditions.

To test this hypothesis, we constructed Δ*myp2 myo2-E1*. Combining *myo2-E1* with Δ*myp2* results in a strain that is temperature sensitive in all media tested (Figure 1B and Table 2). Even in rich media, this strain has a more severe phenotype than either mutant alone. At 25°C, the permissive

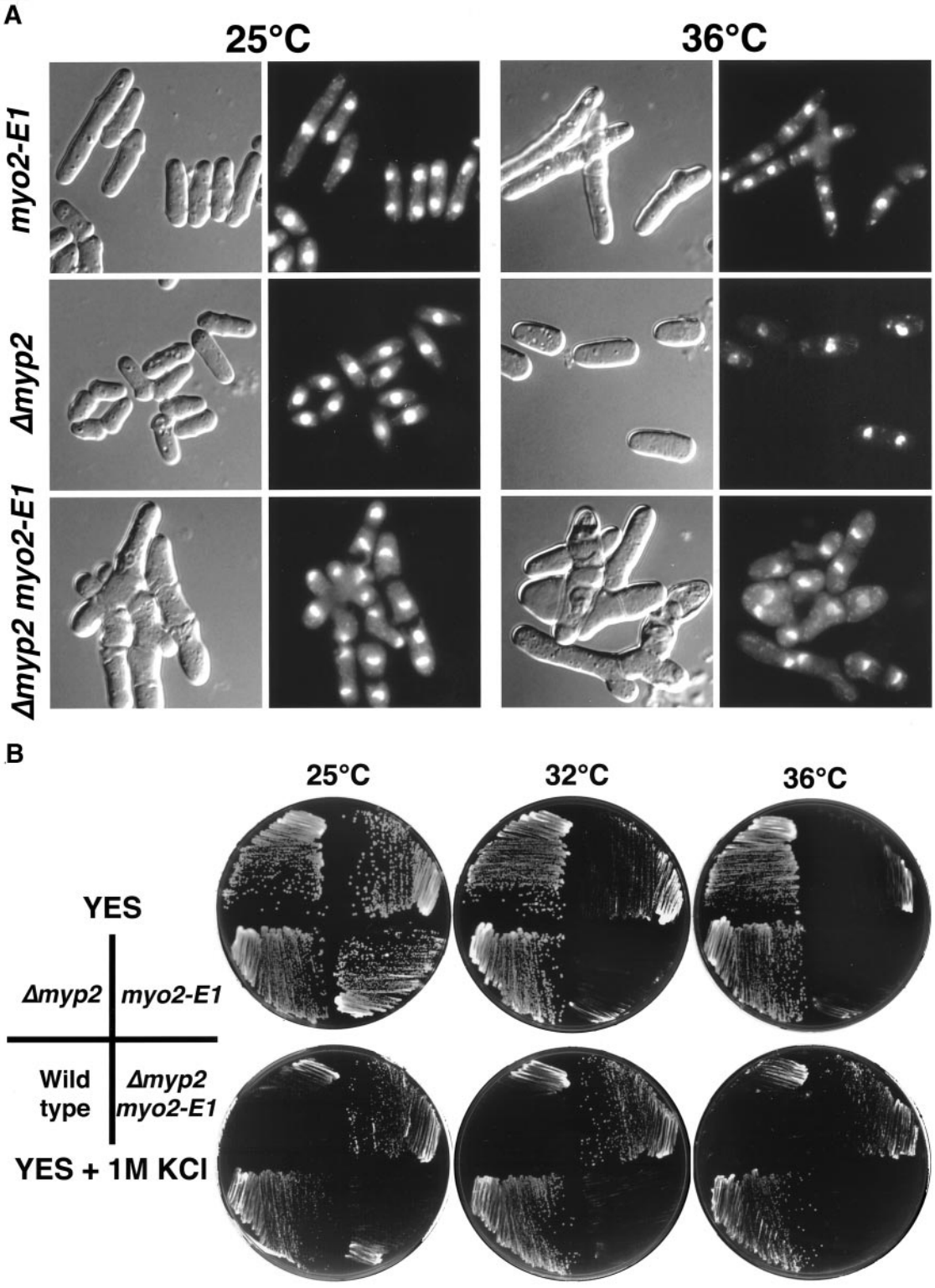


**Figure 1.** Phenotypes of myosin mutant strains. (A) Strains were grown to midlog in YES media at 25°C and then shifted to the indicated temperature for 4 h. The cells were stained with DAPI and visualized by differential interference contrast (left columns) and fluorescence microscopy (right columns). (B) The strains were streaked onto YES plates with or without 1 M KCl and grown at 25, 32, and 36°C.

**Table 2.** Phenotype of strains used in this study

| Strain | Media[a] | 17°C | 25°C | 32°C |
|---|---|---|---|---|
| Wild type | YES | + | + | + |
| Δ*myp2* | YES | + | + | + |
| *myo2-E1* | YES | + | + | −/+ |
| Δ*myp2 myo2-E1* | YES | +/− | +/− | − |
| Wild type | YES + 1 M KCl | + | + | + |
| Δ*myp2* | YES + 1 M KCl | − | sg | sg |
| *myo2-E1* | YES + 1 M KCl | + | + | + |
| Δ*myp2 myo2-E1* | YES + 1 M KCl | − | sg | − |
| Wild type | EMM | + | + | + |
| Δ*myp2* | EMM | + | + | + |
| *myo2-E1* | EMM | + | + | + |
| Δ*myp2 myo2-E1* | EMM | +/− | +/− | − |
| Wild type | EMM + 1 M KCl | + | + | + |
| Δ*myp2* | EMM + 1 M KCl | − | sg | sg |
| *myo2-E1* | EMM + 1 M KCl | + | + | + |
| Δ*myp2 myo2-E1* | EMM + 1 M KCl | − | sg | − |

+, colony formation; +/−, colony is slightly smaller than wild type (stains dark pink with Phloxin B); −/+, formation of microcolonies (stains purple with Phloxin B); −, no colony formation; sg, colony forms slower than wild type.

[a] YES media is rich media. EMM is minimal media.

temperature, cells are elongated, multiseptated, branched, and wider than Δ*myp2* or *myo2-E1* cells (Figure 1A). After 4 h at 36°C, *myo2-E1* arrests as tetranucleate cells usually with one septum. At 36°C Δ*myp2 myo2-E1* cells do not arrest with a uniform morphology; instead, the phenotype observed at 25°C is enhanced, and cell death is evident (Figure 1A). At 25°C, Δ*myp2 myo2-E1* colonies are smaller (Figure 1B) and stain dark pink with Phloxin B, a vital dye expelled by normal cells. Δ*myp2 myo2-E1* is also cold sensitive in 1 M KCl (Table 2).

*myp2*$^+$ probably suppresses *myo2-E1* in certain media, because the protein levels of Myo2p and Myp2p are constant in a *myo2-E1* strain before and after temperature shift (our unpublished results). Also, Myo2p levels are not affected in Δ*myp2 myo2-E1*, and Myp2p protein levels are constant in varying media (our unpublished results). Using temperature-sensitive cell cycle mutants to block the cell cycle at specific stages, we determined that Myp2p and Myo2p protein levels are constant throughout the cell cycle (our unpublished results). We cannot explain any of the phenotypes by variation of expression levels from strain to strain or under varying media conditions. Therefore, we conclude that *myp2*$^+$ and *myo2*$^+$ have unique functions, which allow *S. pombe* to live in a variety of environmental conditions.

### *Myosin Function Is Specified by the Tail*

To identify which regions of the myosins confer gene-specific functions to *myo2*$^+$ and *myp2*$^+$, we tested the ability of chimeric myosins to rescue myosin mutant strains (Figure 2 and Table 3). The chimera Myp2Head Myo2Tail (pHoT) has the head and light chain binding (IQ) motifs of Myp2p attached to the Myo2p tail. The chimera Myo2Head Myp2Tail (oHpT) has the head and IQ motifs of Myo2p attached to the Myp2p tail. To allow expression over a range of levels, the wild-type and chimeric genes were placed under the control of two different *nmt1*$^+$ promoters, a

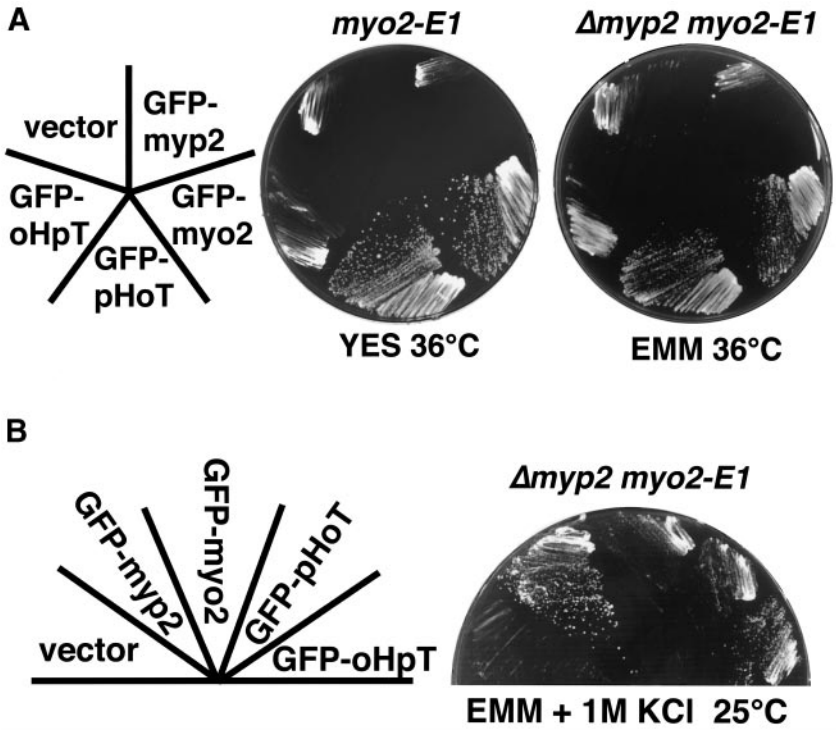


**Figure 2.** Complementation of myosin mutant strains using GFP-myosin fusion constructs. pHoT denotes chimera with Myp2p Head and Myo2p Tail. oHpT denotes chimera with Myo2p Head and Myp2p Tail. (A) Complementation of the temperature sensitivity imparted by the *myo2-E1* allele. The constructs are under the control of the strongest *nmt1*$^+$ promoter, and the vector is marked with *LEU2*. (B) Complementation of the KCl sensitivity imparted by the Δ*myp2* allele. The constructs are under the control of the strongest *nmt1*$^+$ promoter and are marked by *ura4*$^+$.

**Table 3.** Complementation of mutant myosin-II strains

| Strain | Media[a] | Plasmid[b] | 17°C | 25°C | 32°C | 36°C |
|---|---|---|---|---|---|---|
| Δ*myp2* | EMM + 1 M KCl | pGFPLEU2 | − | sg | sg | sg |
| Δ*myp2* | EMM + 1 M KCl | GFP-myp2 | + | + | + | + |
| Δ*myp2* | EMM + 1 M KCl | GFP-myo2 | − | −/+ | sg | sg |
| Δ*myp2* | EMM + 1 M KCl | GFP-pHoT | − | sg | sg | sg |
| Δ*myp2* | EMM + 1 M KCl | GFP-oHpT | + | + | + | + |
| *myo2-E1* | YES | pGFPLEU2 | ND | + | − | − |
| *myo2-E1* | YES | GFP-myp2 | ND | + | − | − |
| *myo2-E1* | YES | GFP-myo2 | ND | + | + | + |
| *myo2-E1* | YES | GFP-pHoT | ND | + | + | + |
| *myo2-E1* | YES | GFP-oHpT | ND | + | − | − |
| Δ*myp2 myo2-E1* | EMM | pGFPLEU2 | ND | + | − | − |
| Δ*myp2 myo2-E1* | EMM | GFP-myp2 | ND | + | −/+ | − |
| Δ*myp2 myo2-E1* | EMM | GFP-myo2 | ND | + | + | + |
| Δ*myp2 myo2-E1* | EMM | GFP-pHoT | ND | + | + | + |
| Δ*myp2 myo2-E1* | EMM | GFP-oHpT | ND | + | +/− | − |
| Δ*myp2 myo2-E1* | EMM + 1 M KCl | pGFPLEU2 | − | sg | − | − |
| Δ*myp2 myo2-E1* | EMM + 1 M KCl | GFP-myp2 | + | + | + | + |
| Δ*myp2 myo2-E1* | EMM + 1 M KCl | GFP-myo2 | − | sg | − | − |
| Δ*myp2 myo2-E1* | EMM + 1 M KCl | GFP-pHoT | − | sg | − | − |
| Δ*myp2 myo2-E1* | EMM + 1 M KCl | GFP-oHpT | + | + | + | + |
| Δ*myo2* | EMM | pGFPLEU2 | ND | ND | − | ND |
| Δ*myo2* | EMM | GFP-myp2 | ND | ND | − | ND |
| Δ*myo2* | EMM | GFP-myo2 | ND | ND | + | ND |
| Δ*myo2* | EMM | GFP-pHoT | ND | ND | + | ND |
| Δ*myp2* | EMM | GFP-oHpT | ND | ND | − | ND |
| Δ*myp2* Δ*myo2* | EMM | pGFPLEU2 | ND | ND | − | ND |
| Δ*myp2* Δ*myo2* | EMM | GFP-myp2 | ND | ND | − | ND |
| Δ*myp2* Δ*myo2* | EMM | GFP-myo2 | ND | ND | + | ND |
| Δ*myp2* Δ*myo2* | EMM | GFP-pHoT | ND | ND | + | ND |
| Δ*myp2* Δ*myo2* | EMM | GFP-oHpT | ND | ND | − | ND |

pHoT denotes chimera with *myp2*$^+$ head and *myo2*$^+$ tail. oHpT denotes chimera with *myo2*$^+$ head and *myp2*$^+$ tail. +, colony formation; −, no colony formation; +/−, colonies of smaller size; −/+, microcolonies; sg, colonies form slower than wild type cells; ND, not determined. Complementation of Δ*myo2* and Δ*myo2* Δ*myp2* accomplished by random spore analysis (see MATERIALS AND METHODS).

[a] YES is rich media. EMM is minimal media.

[b] All constructs under the control of the weakest *nmt1*$^+$ promoter.

weaker promoter and a stronger promoter (see MATERIALS AND METHODS). Either the strongest (Figure 2) or weakest promoters (Table 3) can rescue mutant phenotypes with appropriate myosins under repressed (leaky) expression, whereas they give overexpression phenotypes under nonrepressed conditions (discussed below). We verified that expression levels were comparable for each construct by immunoblotting for the GFP tag (our unpublished results).

Myosins containing the Myo2p Tail, Myo2p and pHoT (Myp2Head Myo2Tail) show identical rescue patterns, only complementing under conditions requiring Myo2p (Table 3). Conversely Myp2p and oHpT (Myo2Head Myp2Tail), myosins containing the Myp2p tail, also show identical rescue patterns, only complementing when Myp2p is required (Table 3). These results strongly suggest that myosin heads, with their associated light chains, have similar functions and that the tails have different functions. In some cases, excess GFP-myo2 can complement loss of *myp2*$^+$ function. However, expression of GFP-myo2 from the weak promoter is not sufficient to complement Δ*myp2* or Δ*myp2 myo2-E1* (Table 3).

Overexpression of either *myp2*$^+$ or *myo2*$^+$ is toxic in wild-type cells (Bezanilla *et al.*, 1997; Kitayama *et al.*, 1997). We find that the overexpression phenotypes of the two myosins are distinct (Figure 3). Using GFP fused to the N terminus of the heads, we visualized the distribution of GFP-myp2 and GFP-myo2 in cells. GFP-myo2 and GFP-myp2 are fully functional in a variety of complementation experiments (Bezanilla *et al.*, 1997; Kitayama *et al.*, 1997). Cells overexpressing Myo2p are fat and elongated but relatively straight and unbranched. Cells overexpressing Myp2p are generally very branched, elongated, and curved. Overexpression of chimeric myosins is also toxic, with the phenotypes determined by the tails, not the heads (Figure 3).

When expressed at relatively low levels, both GFP-tagged wild-type and GFP-tagged chimeric myosins have similar intracellular distributions. The myosins are localized in a spot near the nucleus during interphase and form a ring in the center of the cell during mitosis (Bezanilla *et al.*, 1997; Kitayama *et al.*, 1997). In some cases, GFP-myo2 and GFP-pHoT form multiple spots during interphase, possibly resulting from slightly elevated levels of expression (our unpublished results).

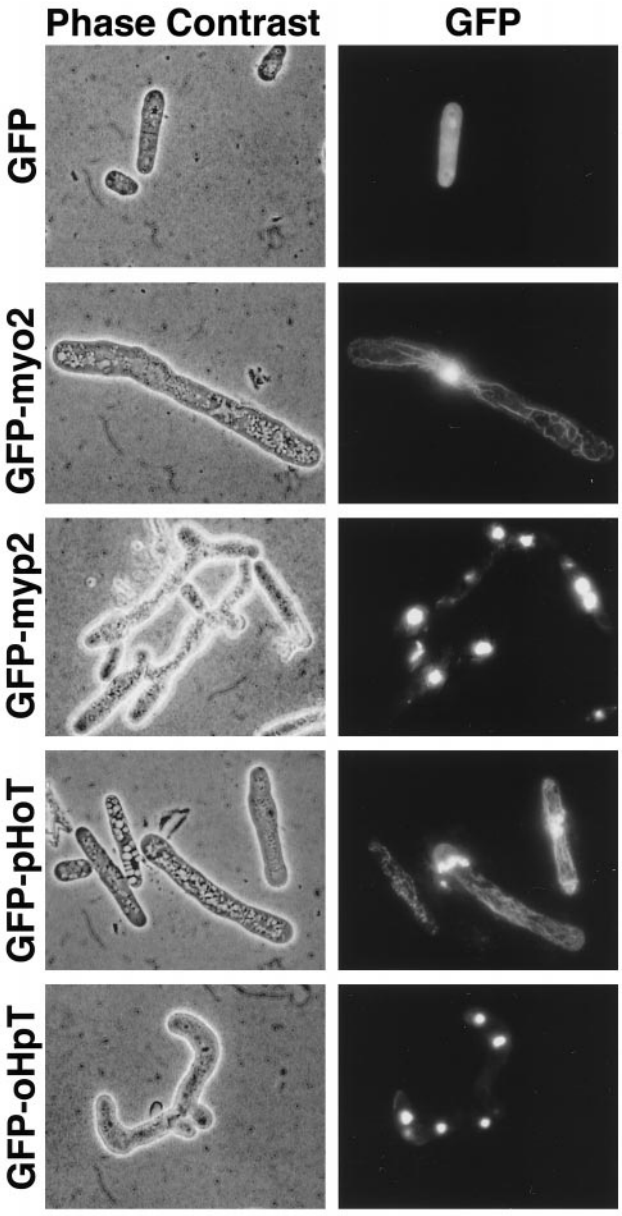


**Figure 3.** Localization of overexpressed GFP-myosin fusion constructs. pHoT denotes chimera with Myp2p Head and Myo2p Tail. oHpT denotes chimera with Myo2p Head and Myp2p Tail. Left column, Phase contrast; right column, GFP fluorescence signal. The overexpression phenotype as well as the localization of the overexpressed protein correlates with the tail of the myosin.

When the myosins are highly overexpressed, localization patterns are distinct before cell death. GFP-myp2 and GFP-oHpT form multiple large aggregates, whereas GFP-myo2 and GFP-pHoT generally have one aggregate per cell with very bright radiating fibrils (Figure 3).

The myosin-II mutant phenotypes show that *myp2*$^+$ and *myo2*$^+$ have nonoverlapping functions. The tails determine whether the myosin will function as *myo2*$^+$ or as *myp2*$^+$.

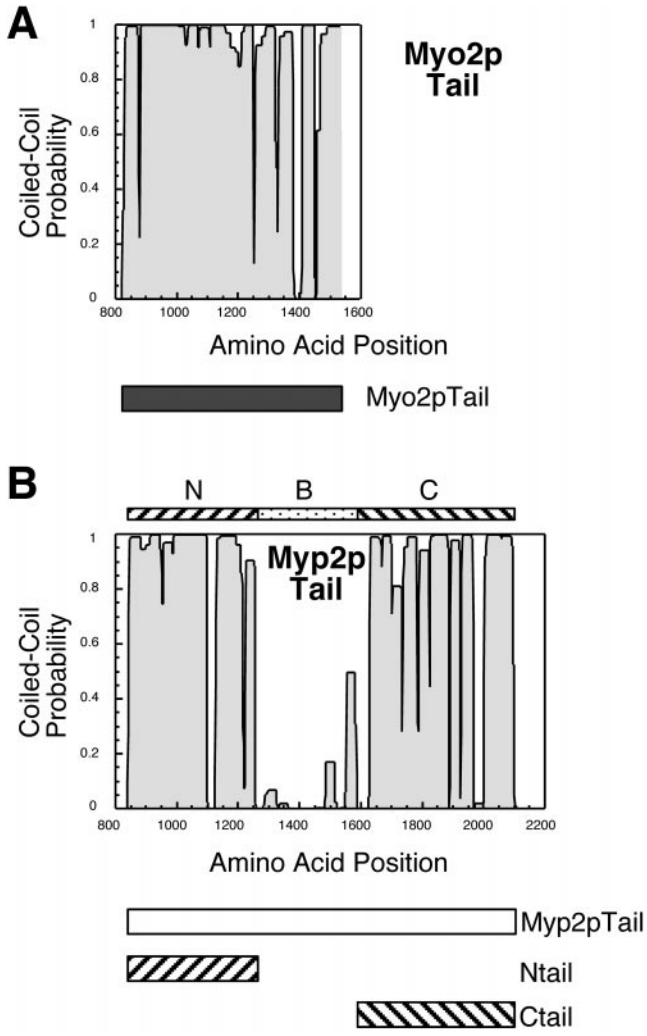


**Figure 4.** Constructs used for physical studies. (A) Coiled-coil prediction (Lupas *et al.*, 1991) of the 711 residue Myo2p Tail. The bar below the graph shows the recombinant tail. (B) Coiled-coil prediction of the 1336 residue Myp2p Tail. The bars above the graph denote the domain structure in the Myp2p Tail. The bars below the graph represent the constructs of the Myp2p Tail used in this study.

Thus we turned our attention to the structural properties of these myosin-II tails that could contribute to these differences.

### *Myp2p and Myo2p Tails Are Structurally Distinct*

All myosin-IIs studied to date have a rod-shaped tail formed by the parallel association of two heavy chains into an alpha-helical coiled coil (Lowey *et al.*, 1969; McLachlan, 1984). These tails allow myosin-IIs to assemble bipolar filaments in a variety of organisms (Trybus, 1991; Sellers *et al.*, 1996). Analysis of the amino acid sequences of Myp2p and Myo2p tails indicates that both have a propensity to form a coiled coil. However, the Myp2p tail has a large gap of ~250 amino acids in the coiled-coil profile (Figure 4).

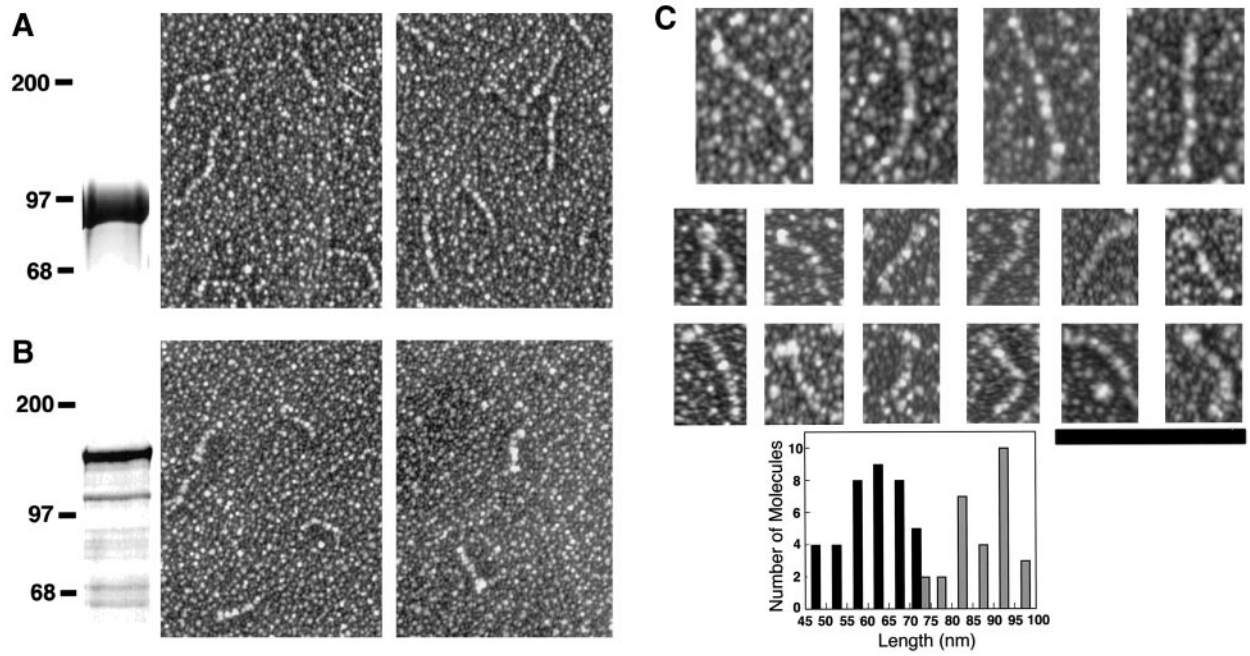


**Figure 5.** (A and B) SDS-PAGE (left) and electron micrographs (right) of purified recombinant Myo2p Tail and Myp2p Tail. For electron microscopy, samples were prepared by rotary shadowing purified proteins in TED buffer with 250 mM NaCl (A) or 500 mM NaCl (B). (A) Purified Myo2p Tail. (B) Purified Myp2p Tail. (C) Magnified electron micrographs of Myo2p Tail (top) and Myp2p Tail (middle). Bottom, Histogram of measured lengths for Myo2p Tail (gray bars) and Myp2p Tail (black bars). Bar in C, 100 nm; refers only to magnified electron micrographs shown in C.

To learn more about the unique functions of these tails, we purified recombinant Myp2p and Myo2p tails from bacteria and studied their properties. Unlike other myosin-II tails (McNally *et al.*, 1991), both *S. pombe* myosin-II tails are insoluble in bacterial lysates. Therefore, we solubilized and purified the recombinant tails in 4 M urea. We refolded the tails by gradual dialysis at low concentrations in a buffer containing high salt to obtain the soluble protein. Both tails are insoluble in low salt, which may represent formation of higher-order structures such as filaments. On SDS-PAGE, Myo2p Tail runs as a single band (Figure 5A, gel), whereas Myp2p Tail is susceptible to proteolysis (Figure 5B, gel). The proteolysis most likely causes nicks in the folded protein, because Myp2p Tail behaves as a single species during sedimentation velocity (our unpublished results) and sedimentation equilibrium ultracentrifugation (Figure 6). N-terminal sequencing of two predominant proteolytic products from the recombinant Myp2p Tail indicates that the nicks occur mainly in the nonhelical region (B; Figure 4). Myp2p is also subject to proteolysis in *S. pombe* cell lysates (our unpublished results).

We assessed the shape of each tail by electron microscopy (Figure 5), the molecular weight and other hydrodynamic parameters in high salt by sedimentation equilibrium analytical ultracentrifugation (Figure 6), and conformation by circular dichroism (CD) spectroscopy (our unpublished results). By all criteria Myo2p Tail is an alpha-helical coiled coil composed of two heavy chains. Myo2p Tail is a single species of 173 kDa in 250 mM NaCl (Figure 6A) and in 100 mM NaCl (our unpublished results), consistent with the formation of a dimer. Below 100 mM NaCl, an increase in light scattering suggests that Myo2p Tail aggregates, possibly forming filaments. By CD spectroscopy Myo2p Tail is >90% alpha-helical in 250 mM NaF (our unpublished results). In the electron microscope, Myo2p Tail prepared by rotary shadowing in 250 mM NaCl is a short rod ~87 nm long (Figure 5A), consistent with a coiled coil composed of 580 residues. Myo2p Tail has 711 residues; however, six of the nine prolines in the tail are concentrated near the end (starting at residue 560 of the tail), lowering the coiled-coil probability to zero (Figure 4A). A coiled coil of 560 residues would be 84 nm long, close to the observed length.

Myp2p Tail has physical properties never before observed for a myosin-II tail. It sediments as a single species of 136 kDa, which is the molecular mass of a monomer (Figure 6B). Electron micrographs of Myp2p Tail prepared by rotary shadowing show a short rod 60 nm long and similar in width to Myo2p Tail (Figure 5B). Approximately half of the rods have a small globular region on one end, possibly representing the nonhelical region (B; Figure 4). Because Myp2p Tail is a monomer, it cannot form a coiled coil consisting of two parallel Myp2p polypeptides, which would be at least 130 nm long. If the two regions of Myp2p Tail predicted to form a coiled coil folded back on themselves in an intramolecular antiparallel coiled coil, the maximum length would be exactly the observed 60 nm. We conclude that Myp2p Tail is a monomeric species with the characteristics of a 60-nm antiparallel coiled-coil rod. If so, Myp2p is the first example of a single-headed myosin-II.

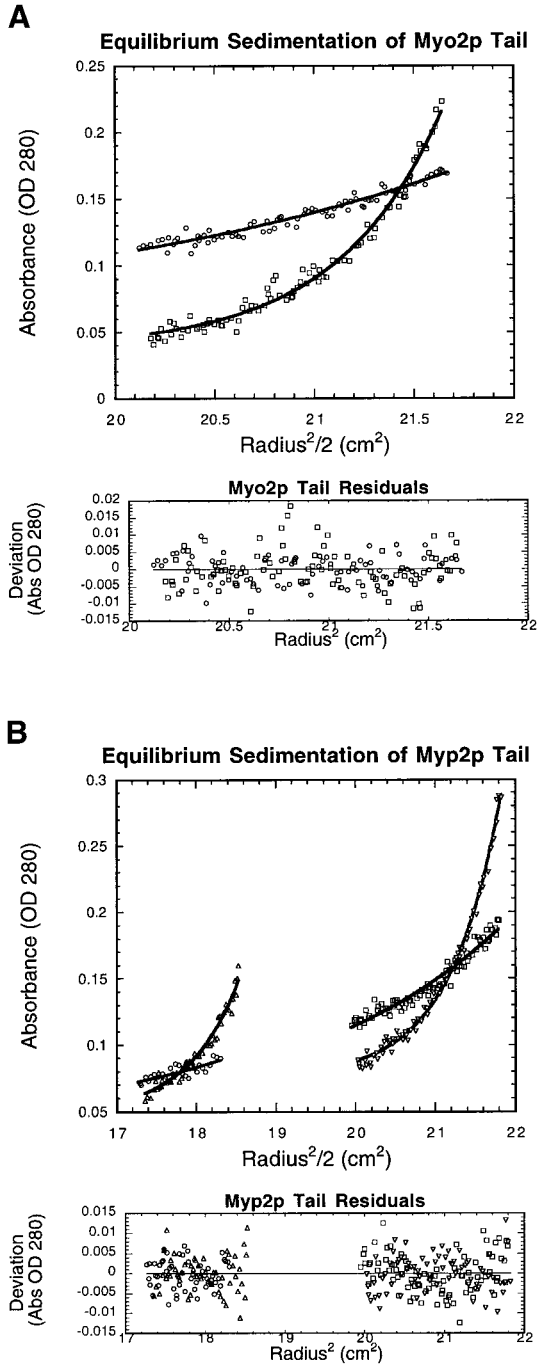


**Figure 6.** Sedimentation equilibrium analysis done at 20°C in TED buffer with 250 mM NaCl (A) or 500 mM NaCl (B). (A) Myo2p Tail, 0.5 mg/ml; circles, 5000 rpm; squares, 10,000 rpm. Lines represent a global fit of the data acquired with the Winonln program. The data were fit by setting the molecular mass to 82 kDa (the polypeptide mass) and floating the association constant for dimerization. The fit results in a $K_d$ of 0.1 nM for the formation of a dimer. Therefore, the major species is a dimer. Fitting for a single species by floating the molecular mass results in a molecular mass of 173 kDa, also consistent with a tightly associated dimer. (B) Myp2p Tail, two concentrations: 0.4 mg/ml (right) and 0.2 mg/ml (left); circles and squares, 5000 rpm; triangles and inverted triangles, 10,000 rpm. Lines represent a global fit of the data acquired with the Winonln program. Fitting for a single species, the data fits best to a molecular mass of 136 kDa. The polypeptide mass is 147 kDa. Attempts to fit a dimer failed. Therefore, recombinant Myp2p Tail is monomeric. Lower graphs in A and B show the deviation of the data from the fit for all data sets.

**Table 4.** Biochemical properties of tail constructs

| Construct | Sedimentation coefficient (S)[a] | Monomeric molecular mass (kDa)[b] | Oligomeric state[c] |
|---|---|---|---|
| Myo2p Tail | 3.5 | 82 | Dimer |
| Myp2p Tail | 3 | 147 | Monomer |
| Myp2p-Ntail | 2.7 | 49 | Dimer |
| Myp2p-Ctail | 1.7 | 58 | Monomer |
| Ntail+Ctail | 2.4 | NA | ND |

[a] Sedimentation coefficient measured by velocity sedimentation analytical ultracentrifugation.

[b] Determined from amino acid composition. NA, not applicable.

[c] Oligomeric state determined by the average molecular mass measured by equilibrium sedimentation analytical ultracentrifugation. ND, not determined.

To test whether Myp2p Tail forms an antiparallel coiled coil, we studied the association of the separately expressed alpha-helical domains. We expressed each alpha-helical domain of the Myp2p tail (Ntail and Ctail; see Figure 4) in bacteria and purified them. On SDS-PAGE Ntail and Ctail run as single bands with the expected molecular mass (Constructs containing the nonhelical region [B] were highly susceptible to proteolysis and therefore not used in these studies.) By sedimentation equilibrium ultracentrifugation, Ctail is a monomer, but Ntail forms a weakly associated dimer (Table 4) with a $K_d$ of 6 $\mu$M. This is very low affinity compared with other myosin-II coiled coils, including Myo2p Tail ($K_d$ = 0.1 nM). Formation of an Ntail-Ctail heterodimer was attempted by refolding Ntail together with Ctail in a 1:1 ratio. Because Ntail forms a weak dimer itself at the concentrations required for sedimentation equilibrium, it is impossible to distinguish between an Ntail-Ctail heterodimer and an Ntail homodimer using this analysis. Thus we used sedimentation velocity to assay formation of an Ntail-Ctail heterodimer. The distribution of sedimentation coefficients for Ntail+Ctail overlaps with Ntail (a homodimer) and is distinct from Ctail (a monomer) (Figure 7). If Ntail and Ctail did not interact, the distribution of sedimentation coefficients would be a broad peak centered between the Ntail and Ctail peaks. Therefore the evidence is consistent with Ntail and Ctail forming a heterodimer, which supports the model of a monomeric Myp2p Tail folding back on itself, resulting in a single-headed myosin-II.

### *The C-terminal Two-Thirds of the Myp2p Tail Are Essential for Its Function*

If the Myp2p tail structure observed in vitro is relevant in vivo, we hypothesized that a C-terminal truncation of

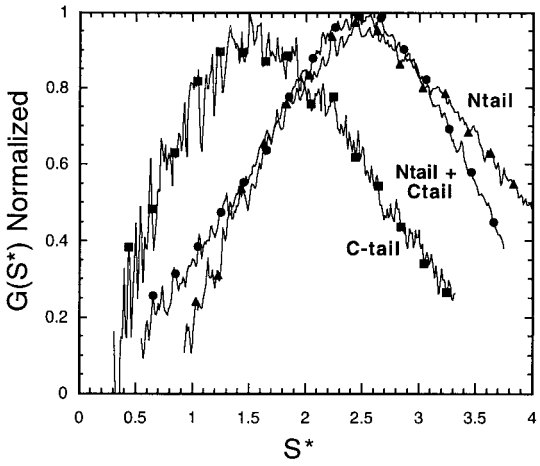


**Figure 7.** Sedimentation velocity analytical ultracentrifugation of Myp2p Tail constructs (Ntail at 0.8 mg/ml, Ctail at 0.4 mg/ml, and Ntail+Ctail at 1.5 mg/ml, total concentration) performed at 20°C in TED buffer with 500 mM NaCl. Distribution of sedimentation coefficients in a sedimentation velocity experiment conducted at 40,000 rpm is shown. Squares, Ctail; triangles Ntail; circles Ntail refolded with Ctail. All sediment as single species. G(S*) is normalized to compare distribution of sedimentation coefficients from samples of varying concentrations.

Myp2p should result in loss of function of *myp2*$^+$. We constructed two disruption constructs of *myp2*$^+$ to remove both the nonhelical region and the C-terminal coiled coil (ΔBC) or just the C-terminal coiled coil (ΔC). We transformed these constructs into wild-type cells and selected for stable integrants. We verified that the *myp2*$^+$ locus was disrupted by PCR (our unpublished results).

Loss of the BC region phenocopies disruption of the entire *myp2*$^+$ locus (Figure 8). Loss of the C region slows growth at 17°C. These data indicate that the B region is essential for *myp2*$^+$ function in 1 M KCl. We were unable to complement Δ*BC* by expressing the BC or C regions; only full-length *myp2*$^+$ can complement Δ*BC* (our unpublished results), implying that an intact tail structure is required. Furthermore, expressing the BC region at low levels (with thiamine) is toxic to Δ*BC* and Δ*myp2* in 1 M KCl at 25 and 17°C (our unpublished results), suggesting that these regions of the protein may titrate away factors required in the absence of functional Myp2p.

Under more normal conditions (in minimal media, EMM, and malt extract) Δ*myp2* also has a slight cytokinesis phenotype (Bezanilla *et al.*, 1997). Both Δ*C* and Δ*BC* exhibit a similar phenotype (our unpublished results). Thus, even though the C region is not absolutely required at 17°C in 1 M KCl, it is required for Myp2p function under more normal conditions.

We also studied the effects of overexpression of various Myp2p tail regions in wild-type cells. Consistent with the disruptions described above, overexpression of the B region or the BC region is toxic to wild-type cells only under conditions in which Myp2p function is required (our unpublished results). Overexpression of the N region has no effect. Therefore, excess amounts of the C-terminal regions of the tail disrupt Myp2p function. Taken together, these data indicate that the structure of the Myp2p tail is important for Myp2p function.

## DISCUSSION

Myosin genes comprise a superfamily defined by their conserved catalytic domains (Mooseker and Cheney, 1995; Sellers *et al.*, 1996). Among this superfamily, myosin-IIs are the best characterized. A defining feature of all known myosin-IIs is their long coiled-coil tail. It is generally acknowledged that myosin-II tails are more divergent in sequence than the catalytic domains (Hammer *et al.*, 1987). The tails all have heptad repeats indicative of a coiled-coil structure, but this does not require a high degree of sequence identity. However, we find that myosin-II tails do contain enough sequence information to classify these myosins into subfamilies. We constructed a phylogenetic tree from the sequences of 34 myosin-II catalytic domains (including the IQ motifs). The catalytic domains grouped into families corresponding to the specialized types of myosin-II (Figure 9A and Table 5). This implies that the sequences of catalytic domains within each family diverged late after organisms separated from each other. These families are well defined, as denoted by the high bootstrapping value observed for the branch points (Figure 9).

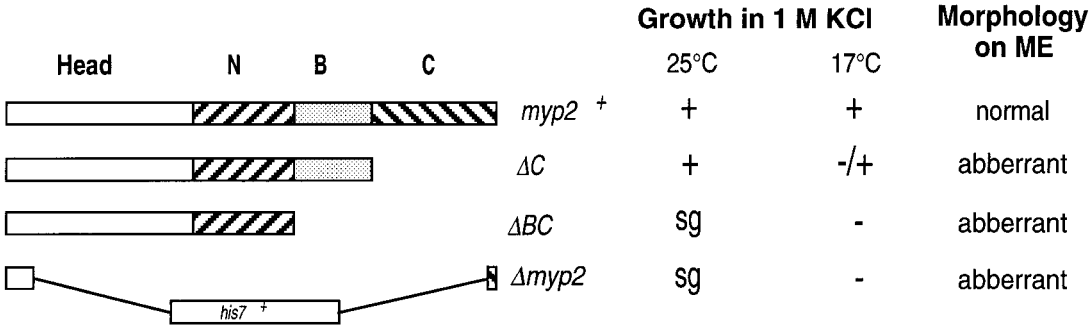


**Figure 8.** Phenotypes of various *myp2*$^+$ deletion strains. The genomic deletions are indicated on the left, and their respective phenotypes in 1 M KCl at 25 and 17°C and in malt extract at 25°C are indicated on the right (+, colony formation is wild type; −/+, microcolony formation; sg, colonies form several days after wild type; −, no colony formation).

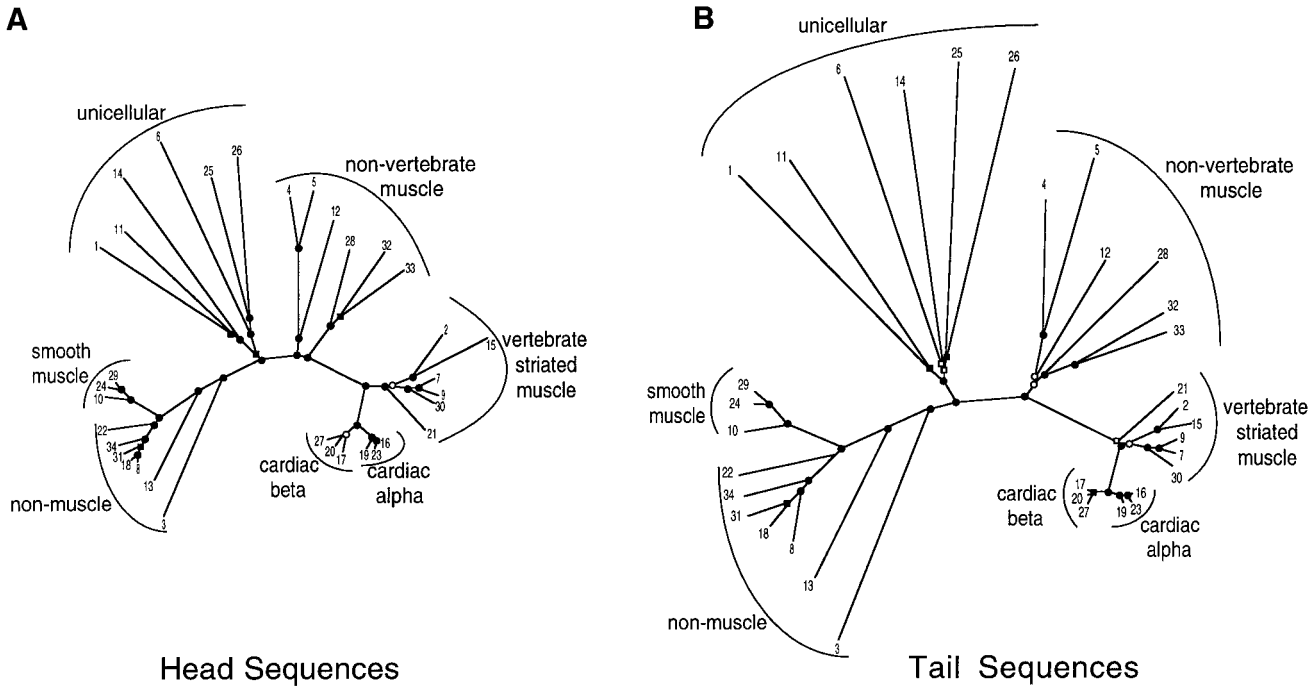


**Figure 9.** Phylogenetic analysis of myosin-II sequences. Both are unrooted trees drawn to the same scale. (A) Tree built from alignment of the head sequences. (B) Tree built from alignment of the tail sequences. Filled circles represent >90% bootstrapping value; filled squares represent 75–90% bootstrapping value; open circles represent 50–75% bootstrapping value; open squares represent 20–50% bootstrapping value. Sequences are numbered and listed in Table 5.

We then built a tree from an alignment of tail sequences of these 34 myosin-IIs. We chose the beginning of the tail to be the invariant proline downstream of the IQ motifs. We were surprised that the tail tree is almost identical to the tree built from the catalytic domains (Figure 9B and Table 5). The main difference is the length of the branches; the head tree has shorter branches than the tail tree, probably owing to less overall sequence similarity among the tails than the heads. Tails have diverged more than catalytic domains, yet tails evolved along with the heads, and tails can be used to classify the type of myosin-II.

The two *S. pombe* myosin-II genes fall into the broad classification of unicellular myosin-IIs. We characterized the phenotypes of strains with mutant myosin-IIs and observed that each myosin has a unique and essential function for viability of the cell under different conditions. By constructing chimeric myosins, we found that the tail determines the identity of the myosin and confers gene-specific functions to each myosin.

The structural properties of the myosin-II tails from *S. pombe* are quite different. Although the Myo2p tail is a conventional coiled-coil rod, which assembles in low salt, the Myp2p tail is unlike any other myosin-II tail studied to date. Although the Myp2p tail sequence is long (1336 residues), the Myp2p tail construct is only 60 nm long. The sequence has a predicted gap in the coiled coil. The two coiled-coil domains have virtually identical coiled-coil prediction profiles. However the Ntail region dimerizes weakly, whereas Ctail does not. Nevertheless, in agreement with the structure observed for the full-length Myp2p tail, when Ntail and Ctail are refolded together, they form a heterodimer. Studies using chymotryptic rod fragments of embryonic, neonatal, and adult myosin-IIs from chicken pectoralis major muscle showed that denaturing and refolding equimolar ratios of different tail isoforms only produced homodimers of one specific isoform (Kerwin and Bandman, 1991). Therefore, refolding Myp2p tail and Myp2p tail subdomains is likely to lead to the correct state. Thus, our data are consistent with a model in which the two predicted coiled-coil domains associate with one another to form an antiparallel coiled coil, making Myp2p the first monomeric myosin-II. Although unprecedented for myosin-IIs, there are two well-documented cases involving antiparallel coiled coils. The cytoplasmic domain of a bacterial serine chemotaxis receptor forms two 20-nm-long antiparallel coiled coils (Kim *et al.*, 1999). The structural maintenance of chromosomes proteins and their related bacterial MukB proteins form even longer antiparallel coiled coils, 40 nm in length (Melby *et al.*, 1998).

Forming an antiparallel coiled coil does not preclude Myp2p from polymerizing into filaments. Like all characterized myosin-II tails, Myp2p Tail is insoluble in low salt. The ability to form Myp2p-specific filaments in the cell may require this unusual tail structure. We are not sure what structure the Myp2p tail adopts in vivo; however, our in vivo studies demonstrate that the C-terminal two-thirds of the Myp2p tail are essential for *myp2*$^+$ function, suggesting that an intact tail structure is required. The nonhelical region B is required for the KCl phenotype; this region is proteo-

**Table 5.** Myosin-II sequences used for phylogenetic analysis

| Sequence | Organism | Tissue/gene or protein name | Sequence ID |
|---|---|---|---|
| 1 | *Acanthamoeba* | Myosin-II | gil127758 |
| 2 | *Cyprinus carpio* (common carp) | Fast skeletal muscle | gil2351223 |
| 3 | *C. elegans* | Nonmuscle | gil1477559 |
| 4 | *C. elegans* | Body wall muscle/myosin heavy chain B | gil127743 |
| 5 | *C. elegans* | Pharyngeal muscle/myosin heavy chain D | gil127751 |
| 6 | *S. cerevisiae* | Myo1p | gil730092 |
| 7 | Chicken | Embryonic skeletal muscle | gil1346637 |
| 8 | Chicken | Nonmuscle | gil104780 |
| 9 | Chicken | Skeletal muscle | gil127766 |
| 10 | Chicken | Smooth muscle | gil86369 |
| 11 | *Dictyostelium* | Myosin-II | gil127774 |
| 12 | *Drosophila* | Embryonic muscle | gil547964 |
| 13 | *Drosophila* | Nonmuscle | gil2119295 |
| 14 | *Entamoeba* | Myosin-II | gil1850913 |
| 15 | *Theragra chalcogramma* (fish) | Skeletal muscle (only heavy meromyosin) | gil3668187 |
| 16 | Hamster | Cardiac alpha | gil402374 |
| 17 | Hamster | Cardiac beta | gil402372 |
| 18 | Human | Nonmuscle myosin A | gil547970 |
| 19 | Human | Cardiac alpha | gil3041706 |
| 20 | Human | Cardiac beta | gil547966 |
| 21 | Human | Embryonic fast skeletal | gil3043372 |
| 22 | Human | Nonmuscle myosin B | gil1346640 |
| 23 | Mouse | Cardiac alpha | gil3024204 |
| 24 | Mouse | Smooth muscle | gil1945080 |
| 25 | *S. pombe* | Myo2p | gil1763304 |
| 26 | *S. pombe* | Myp2p | gil2731818 |
| 27 | Pig | Cardiac beta | gil1698895 |
| 28 | *Dugesia japonica* (planarian) | Muscle | gil3986196 |
| 29 | Rabbit | Smooth muscle | gil1346644 |
| 30 | Rabbit | Skeletal muscle | gil940233 |
| 31 | Rat | Nonmuscle | gil111999 |
| 32 | *Placopecten magellanicus* (scallop) | Striated muscle | gil1408192 |
| 33 | *Loligo pealei* (squid) | Ventral siphon muscle | gil3252880 |
| 34 | *Xenopus* | Nonmuscle | gil3660672 |

lytically sensitive and contains two consensus *cdc2*$^+$ phosphorylation motifs, suggesting it is functionally important.

The unusual structure of the Myp2p tail may be required to activate Myp2p during a stress response, when *myp2*$^+$ is essential. This could be accomplished by removing the C region by proteolysis (unlikely, because $\Delta C$ is less functional under these conditions), by phosphorylation of the nonhelical region B, or by a protein that binds the B region. Excess B region could titrate away this interacting protein, thus disrupting *myp2*$^+$ function, consistent with our overexpression data. Our results also suggest that the C-terminal two-thirds of the tail may interact with the general cytokinesis machinery (see Figure 8 and RESULTS).

To date, only one other myosin-II, *S. cerevisiae* Myo1p, has a predicted tail structure similar to Myp2p (Bezanilla *et al.*, 1997). Myo1p is the only budding yeast myosin-II, and it is not essential. However, deletion of the *S. cerevisiae* myosin-II gene leads to defects in cytokinesis (Watts *et al.*, 1987), reminiscent of the $\Delta$*myp2* phenotype in *S. pombe* (this work; Bezanilla *et al.*, 1997). Cell division in *S. cerevisiae* requires formation of a bud and directed transport of intracellular components into the bud. *S. cerevisiae* has apparently lost the gene for the conventional myosin-II required for cell division in other eukaryotes but has retained the unconventional Myp2-like myosin.

In contrast, *S. pombe* has retained genes for both classes of myosin-II. Thus, *myp2*$^+$ may be required for steps specific to yeast cytokinesis, whereas the more conventional *myo2*$^+$ is required for contraction of the cleavage furrow as in other eukaryotes lacking a cell wall. Yeast cytokinesis is unusual, because it also involves septation. Yeast-specific myosin-IIs such as Myp2p may be required for recruiting septal material or signaling for the septation machinery. This is consistent with genetic interactions between $\Delta$*myp2* and septation mutants (Bezanilla *et al.*, 1997). However, comparison of tail sequences was unable to separate unconventional Myp2p-like myosin-IIs from more conventional myosin-IIs in unicellular organisms, possibly because of the small number of myosin-II sequences from unicellular organisms. Yet our results indicate that differences between Myp2p and Myo2p tails are functionally and structurally significant.

To understand how *S. pombe* regulates cytokinesis, it will be important to understand the biochemical properties of the molecules involved in contraction of the cleavage furrow. Identifying components that interact with Myp2p tail genetically or biochemically will help address the specific role of this unusual myosin-II during cytokinesis in fission yeast.

## ACKNOWLEDGMENTS

We are indebted to Susan L. Forsburg and members of the Forsburg laboratory for providing valuable advice on experimental technique and design. We thank Pamela Maupin for expert technical assistance with electron microscopy and Steven C. Koerber for assistance with CD spectroscopy. We are grateful to Russell F. Doolittle for expert advice regarding the phylogenetic analysis. We thank Sally G. Pasion for the gift of pSGP573 and Susan L. Forsburg for the gift of pTZura4. We thank Michael B. McKeown, Susan L. Forsburg, and members of the Pollard and Forsburg laboratories for critical reading of the manuscript. This work was supported by grant GM-26132 from the National Institutes of Health.

## REFERENCES

Balasubramanian, M.K., McCollum, D., Chang, L., Wong, K.C., Naqvi, N.I., He, X., Sazer, S., and Gould, K.L. (1998). Isolation and characterization of new fission yeast cytokinesis mutants. Genetics *149*, 1265–1275.

Basi, G., Schmid, E., and Maundrell, K. (1993). TATA box mutations in the *Schizosaccharomyces pombe nmt1* promoter affect transcription efficiency but not the transcription start point or thiamine repressibility. Gene *123*, 131–136.

Bezanilla, M., Forsburg, S.L., and Pollard, T.D. (1997). Identification of a second myosin-II in *Schizosaccharomyces pombe*: Myp2p is conditionally required for cytokinesis. Mol. Biol. Cell *8*, 2693–2705.

Fishkind, D.J., and Wang, Y.L. (1995). New horizons for cytokinesis. Curr. Opin. Cell Biol. *7*, 23–31.

Hammer, J.D., Bowers, B., Paterson, B.M., and Korn, E.D. (1987). Complete nucleotide sequence and deduced polypeptide sequence of a nonmuscle myosin heavy chain gene from *Acanthamoeba*: evidence of a hinge in the rodlike tail. J. Cell Biol. *105*, 913–925.

Huxley, H.E., and Brown, W. (1967). The low-angle x-ray diagram of vertebrate striated muscle and its behavior during contraction and rigor. J. Mol. Biol. *30*, 383–434.

Javerzat, J.P., Cranston, G., and Allshire, R.C. (1996). Fission yeast genes which disrupt mitotic chromosome segregation when overexpressed. Nucleic Acids Res. *24*, 4676–4683.

Johnson, M.L., Correia, J.J., Yphantis, D.A., and Halvorson, H.R. (1981). Analysis of data from the analytical ultracentrifuge by nonlinear least-squares techniques. Biophys. J. *36*, 575–588.

Kerwin, B., and Bandman, E. (1991). Assembly of avian skeletal muscle myosins: evidence that homodimers of the heavy chain subunit are the thermodynamically stable form. J. Cell Biol. *113*, 311–320.

Kim, K.K., Yokota, H., and Kim, S.H. (1999). Four-helical-bundle structure of the cytoplasmic domain of a serine chemotaxis receptor. Nature *400*, 787–792.

Kitayama, C., Sugimoto, A., and Yamamoto, M. (1997). Type II myosin heavy chain encoded by the *myo2* gene composes the contractile ring during cytokinesis in *Schizosaccharomyces pombe*. J. Cell Biol. *137*, 1309–1319.

Liang, D.T., Hodson, J.A., and Forsburg, S.L. (1999). Reduced dosage of a single fission yeast MCM protein causes genetic instability and S phase delay. J. Cell Sci. *112*, 559–567.

Lowey, S., Slayter, H.S., Weeds, A.G., and Baker, H. (1969). Substructure of the myosin molecule. I. Subfragments of myosin by enzymic degradation. J. Mol. Biol. *42*, 1–29.

Lupas, A., Van Dyke, M., and Stock, J. (1991). Predicting coiled-coils from protein sequences. Science *252*, 1162–1164.

Mabuchi, I., and Okuno, M. (1977). The effect of myosin antibody on the division of starfish blastomeres. J. Cell Biol. *74*, 251–263.

May, K.M., Watts, F.Z., Jones, N., and Hyams, J.S. (1997). Type II myosin involved in cytokinesis in the fission yeast *Schizosaccharomyces pombe*. Cell Motil. Cytoskeleton *38*, 385–396.

McLachlan, A.D. (1984). Structural implications of the myosin amino acid sequence. Annu. Rev. Biophys. Bioeng. *13*, 167–189.

McNally, E., Sohn, R., Frankel, S., and Leinwand, L. (1991). Expression of myosin and actin in *Escherichia coli*. Methods Enzymol. *196*, 368–389.

Melby, T.E., Ciampaglio, C.N., Briscoe, G., and Erickson, H.P. (1998). The symmetrical structure of structural maintenance of chromosomes (SMC) and MukB proteins: long, antiparallel coiled-coils, folded at a flexible hinge. J. Cell Biol. *142*, 1595–1604.

Mooseker, M.S., and Cheney, R.E. (1995). Unconventional myosins. Annu. Rev. Cell Dev. Biol. *11*, 633–675.

Moreno, S., Klar, A., and Nurse, P. (1991). Molecular genetic analysis of fission yeast *Schizosaccharomyces pombe*. Methods Enzymol. *194*, 795–823.

Motegi, F., Nakano, K., Kitayama, C., Yamamoto, M., and Mabuchi, I. (1997). Identification of Myo3, a second type-II myosin heavy chain in the fission yeast *Schizosaccharomyces pombe*. FEBS Lett. *420*, 161–166.

Okazaki, K., Okazaki, N., Kume, K., Jinno, S., Tanaka, K., and Okayama, H. (1990). High-frequency transformation method and library transducing vectors for cloning mammalian cDNAs by trans-complementation of *Schizosaccharomyces pombe*. Nucleic Acids Res. *18*, 6485–6489.

Pollard, T.D. (1982). Structure and polymerization of *Acanthamoeba* myosin-II filaments. J. Cell Biol. *95*, 816–825.

Satterwhite, L.L., and Pollard, T.D. (1992). Cytokinesis. Curr. Opin. Cell Biol. *4*, 43–52.

Sellers, J.R., Goodson, H.V., and Wang, F. (1996). A myosin family reunion. J. Muscle Res. Cell Motil. *17*, 7–22.

Sinard, J.H., and Pollard, T.D. (1989). The effect of heavy chain phosphorylation and solution conditions on the assembly of *Acanthamoeba* myosin-II. J. Cell Biol. *109*, 1529–1535.

Tommasino, M., and Maundrell, K. (1991). Uptake of thiamine by *Schizosaccharomyces pombe* and its effect as a transcriptional regulator of thiamine-sensitive genes. Curr. Genet. *20*, 63–66.

Trybus, K.M. (1991). Assembly of cytoplasmic and smooth muscle myosins. Curr. Opin. Cell Biol. *3*, 105–111.

Watts, F.Z., Shiels, G., and Orr, E. (1987). The yeast *MYO1* gene encoding a myosin-like protein required for cell division. EMBO J. *6*, 3499–3505.

Way, M., Pope, B., Gooch, J., Hawkins, M., and Weeds, A.G. (1990). Identification of a region in segment 1 of gelsolin critical for actin binding. EMBO J. *9*, 4103–4109.